Supplementary Materials and Methods

Animal Experiments

CN2, *irf-1*$^{-/-}$, and *irf-9*$^{-/-}$ mice were maintained in conventional animal housing under specific pathogen-free conditions. AxCANCre and AxCAw1, which are replication-deficient recombinant adenoviruses that lack the E1A, E1B, and E3 regions, were obtained from Dr Izumu Saito (University of Tokyo).[1] AxCANCre expresses the Cre recombinase, whereas AxCAw1, which was used as a control, lacks the inserted *cre* gene. The Cre-expressing recombinant adenovirus (AxCANCre) and AxCAwl were expanded in HEK293 cells (kindly gifted by Dr Izumu Saito) and purified by sucrose gradient centrifugation.[1] AxCANCre or AxCAw1 (2×10^9 plaque-forming units) was injected intravenously into CN2 or nontransgenic female mice aged 9–13 weeks. The mice were killed at 4, 7, 10, 14, 21, 60, 90, 180, 400, 500, or 600 days after injection (n = 15 mice/group; total of 900 mice). Mouse behavior and phenotypes were assessed weekly, and the phenotypes were confirmed at necropsy. At necropsy, the proportion of mice with enlarged lymph nodes, according to weight, was larger in the CN2 group than in the WT group ($P < .05$). To elicit Fas-induced liver damage, adult mice were injected intravenously with 10 μg of an anti-mouse Fas monoclonal antibody that was purified from a hamster (clone Jo2; Pharmingen) in 200 μL phosphate-buffered saline (without Ca^{2+} or Mg^{2+}). Animals were observed over a 24-hour period for survival or killed at matched time points; livers were collected for histology or biochemical studies. All the animal experiments were performed according to the guidelines of the Tokyo Metropolitan Institute of Medical Science Subcommittee for Laboratory Animal Care. The protocol was approved by an institutional review board.

For CN2-29 Mx1-Cre mice, Cre expression in the liver was induced by intraperitoneal injection of poly(I:C) (GE Healthcare UK Ltd, Buckinghamshire, England). A total of 300 μL of poly(I:C) solution (1 mg/mL in phosphate-buffered saline) was injected 3 times at 48-hour intervals.

Southern Blot Analysis

Mouse livers were digested overnight at 55°C in lysis buffer (50 mmol/L Tris-HCl [pH 7.6], 100 mmol/L NaCl, 20 mmol/L EDTA, 1% sodium dodecyl sulfate) that contained 1 mg/mL proteinase K (Boehringer Mannheim, Mannheim, Germany). DNA was extracted with phenol-chloroform and precipitated with ethanol.[1] The DNA pellet was washed with 70% ethanol, dried, and resuspended in 10 mmol/L Tris (pH 7.5). Restriction endonuclease digestion with XbaI, agarose gel electrophoresis, and Southern blotting were performed using the DIG DNA Labeling and Detection System (Boehringer Mannheim). XbaI-mediated DNA fragmentation was used to examine the rate of recombination of the HCV transgene construct.[1] Recombination of the transgene (CN2) was confirmed by Southern blotting. Southern blotting of DNA samples extracted from mouse livers was performed using the DIG DNA Labeling and Detection System (Boehringer Mannheim).

Quantification of HCV Core Protein in Mouse Livers

Mouse livers were homogenized in 1 mL RIPA buffer (1% sodium dodecyl sulfate, 0.5% [vol/vol] Nonidet P40, 10 mmol/L Tris [pH 7.4], 0.15 mol/L NaCl). The HCV core protein concentrations in the liver lysates were quantified using a fluorescent enzyme immunoassay with 2 high-affinity monoclonal antibodies against the HCV core protein.[2] The HCV core protein concentration in each liver was normalized by the total protein concentration, as measured using the DC protein assay (Bio-Rad Laboratories, Hercules, CA).

Collection of Sera and Enzyme-Linked Immunosorbent Assay

To assess Fas-induced liver failure, blood samples were collected from the supraorbital veins at 0, 1, 2, 3, 4, 5, and 6 hours after administration of the Fas monoclonal antibody or by heart puncture of killed mice. Blood samples were centrifuged at 10,000*g* for 15 minutes at 4°C to isolate serum. The serum levels of IL-2, IL-4, IL-10, and IL-12 were determined using enzyme-linked immunosorbent assay kits (R&D Systems, Minneapolis, MN), according to the manufacturer's instructions. Serum alanine aminotransferase (ALT) activity was determined using a commercially available kit (Nissui, Tokyo, Japan).

Histology and Immunohistochemical Staining

Livers were frozen in Tissue-Tek OCT compound (SAKURA Finetek, Tokyo, Japan) in dry ice/ethanol, thawed, and fixed in 1:1 (vol/vol) acetone/methanol at −20°C for 10 minutes. Immunohistochemical staining was completed using tyramide signal amplification (NEN Life Science Products, Boston, MA). Nuclei were stained with 0.5 μg/mL Hoechst 33342 (Molecular Probes, Carlsbad, CA) for 1 minute at room temperature. Sections were observed under a fluorescence microscope (510 Meta; Carl Zeiss, Oberkochen, Germany). Liver samples for histology were cut into small (<1.0 cm) pieces, fixed overnight in 10% paraformaldehyde, dehydrated with ethanol, blocked in paraffin, sectioned at 10-μm thickness, stained with H&E, and viewed under a microscope (510 Meta; Carl Zeiss). For HCV core protein detection, immunohistochemistry was performed using PFA-fixed or OCT frozen sections. Tissue sections were fixed in 4% PFA and permeabilized in 0.3% H_2O_2 and methanol for 10 minutes. Antigen retrieval was achieved by autoclaving at 121°C for 5 minutes or 10 minutes or by treatment with proteinase K at 37°C for 10 minutes or 30 minutes. To detect core antigen, a mouse anti-core antibody (BT 515) and Alexa 488–conjugated streptavidin were used.

Staining was detected by the DAB substrate reaction. For CD3 and CD45R protein detection, immunohistochemistry was performed on PFA-fixed sections. Tissue sections were fixed with 4% PFA and permeabilized by treating with 0.3% H_2O_2 and methanol for 10 minutes. Antigen retrieval was achieved by autoclaving at 121°C for 10 minutes. To detect the CD3 and CD45R antigens, mouse anti-CD3 and anti-CD45R antibodies (AbD Serotec MorphoSys UK Ltd, Oxford, England) were used. Staining was detected by the addition of 3,3′-diaminobenzidine tetroxide (Dojin Kagaku, Kumamoto, Japan).

Flow Cytometry

Lymphocytes were stained with appropriate dilutions of the following antibodies: PE-conjugated anti-CD3, fluorescein isothiocyanate (FITC)-conjugated anti-B220, FITC-conjugated anti-CD4, PE-conjugated anti-CD8, FITC-conjugated anti–TCR-$\alpha\beta$, and PE-conjugated anti–TCR-$\gamma\delta$. Flow cytometry was performed using the FACSCalibur (Becton Dickinson, San Jose, CA).

Western Blot Analysis

Minced livers, lymph nodes, spleens, and splenocytes were homogenized with a Dounce glass homogenizer at 4°C in lysis buffer (1% bovine serum albumin, 1 mmol/L ethylene glycol-bis[2-aminoethylether]-*N,N,N′N′*-tetraacetic acid, 300 mmol/L sucrose, 5 mmol/L 3-[N-morpholino]propanesulfonic acid, 5 mmol/L KH_2PO_4 [pH 7.4]) that contained complete protease inhibitor cocktail (Boehringer Mannheim). After centrifugation at 27,000*g* for 15 min, 50 μg of supernatant protein were loaded in each lane of a 10% or 15% polyacrylamide gel, separated by electrophoresis in Tris-Tricine buffer (Daiichi Pure Chemicals), and transferred to polyvinylidene difluoride membranes (Amersham Life Science, Tokyo, Japan). The membranes were then incubated for 2 hours at room temperature in TBS-T (20 mmol/L Tris-HCl, 500 mmol/L NaCl, 0.1% [vol/vol] Tween 20) that contained 1% bovine serum albumin, followed by incubation with a primary antibody directed against Bcl-2 (Santa Cruz Biotechnology, Santa Cruz, CA), protein kinase R (a kind gift of Dr H. Taira, Iwate University, Japan), mouse IRF-1 (Santa Cruz Biotechnology), mouse Fas (Wako), or HCV core (31-2).[3] The membranes were washed with TBS-T, incubated with horseradish peroxidase–conjugated secondary antibodies, visualized using a chemiluminescence reagent (Amersham International, Tokyo, Japan), and detected using Hyperfilm-MP (Amersham International).

Detection of Apoptotic Cells by DNA Fragmentation

Small pieces of liver (50–80 mg in weight) were homogenized and digested overnight with proteinase K (Boehringer Mannheim) at 55°C in lysis buffer (50 mmol/L Tris-HCl [pH 7.6], 100 mmol/L NaCl, 20 mmol/L EDTA, 1% sodium dodecyl sulfate). Lysates were extracted with phenol-chloroform-isoamyl alcohol, treated with ribonuclease, precipitated with ethanol, and subjected to 2% agarose gel electrophoresis. Breaks in the hepatocyte DNA were detected using the terminal deoxynucleotidyl transferase–mediated deoxyuridine triphosphate nick-end labeling (TUNEL) assay kit (R&D Systems) according to the manufacturer's instructions.

Ribonuclease Protection Assay

The caspase transcript levels in the livers from *irf-1*$^{-/-}$ and *irf-1*$^{+/+}$ mice were determined in a ribonuclease protection assay that used mouse apoptosis multiprobe template sets (Pharmingen). Briefly, total RNA was extracted from the livers and assayed with the RiboQuant Multi-Probe RNase Protection Assay System mAPO-1 (Becton Dickinson). Multiple ^{32}P-labeled caspase probes and the control glyceraldehyde-3-phosphate dehydrogenase probe were synthesized and hybridized overnight to the target RNA, treated with ribonuclease, and separated by electrophoresis on a denaturing polyacrylamide gel. The radioactive bands representing undigested RNAs were then detected and quantified using the BAS 2000 phosphoimager (Fuji Photo Film, Tokyo, Japan). Band intensities were normalized to the glyceraldehyde-3-phosphate dehydrogenase mRNA band in the same lane.

RNA Isolation and Reverse-Transcription PCR

The mRNA species from mouse splenocytes and peripheral blood lymphocytes were isolated using Isogen (Nippon Gene, Shizouka, Japan). The core, E1, E2, NS2, and lacZ mRNA species were detected by reverse-transcription PCR using the following primers: for core-621S, 5′-gggcaggatggctcctgtca-3′; for core-831A, 5′-ttcacgccgtcctccacaac-3′; for E1-991S, 5′-agcggacatgatcatgcata-3′; for E1-1314A, 5′-atcatcatgtcccaagccat-3′; for E2-1601S, 5′-tggcacatcaacaggactgc-3′; for E2-1860A, 5′-actggaccacacaccttcga-3′; for NS2-2807S, 5′-gtgtttgtaggtctggtact-3′; for NS2-2925A, 5′-atccacacttgcaggtgcgc-3′; for lacZ 30S, 5′-aaccctggcgttacccaact-3′; and for lacZ 430A, 5′-gaaacgccgagttaacgcca-3′.

Quantitative Real-Time PCR Amplification of Cytokine and Bcl-2 mRNA Species

The RNA from 10,000 cells was used for art-PCR in the ABI Prism 7900-HT Sequence Detection System with the Universal PCR Master Mix (Applied Biosystems, Foster City, CA) and the RT2 qPCR Primer sets for murine IL-2, IL-4, IL-10, IL-12, *bcl-2,* and glyceraldehyde-3-phosphate dehydrogenase (SABioscience Inc, Frederick, MD; and Applied Biosystems), as described previously.[4] The quantitative real-time PCR results are presented as the average values from at least 3 independent experiments with duplicate PCR analyses.

Measurements of Caspase Activities Through Cleavage of Fluorogenic Substrates

The cytosolic fractions of splenocytes were isolated as described previously,[5] with some modifications. Briefly, splenocytes were homogenized in a Dounce glass homogenizer (loose type) with lysis buffer (0.3 mol/L mannitol, 5 mmol/L 3-[*N*-morpholino]propanesulfonic acid, 1 mmol/L ethylene glycol-bis[β-aminoethyl ether]-*N*,*N*,*N*′,*N*′-tetraacetic acid, 4 mmol/L KH_2PO_4, 20 μg/mL leupeptin, 10 μg/mL pepstatin A, 10 μg/mL aprotinin, 2 mmol/L phenylmethylsulfonyl fluoride) and fractionated into pellet, heavy membrane, light membrane, and cytosolic fractions. The lysates were centrifuged at 600*g* for 10 minutes at 4°C to remove debris or fibers. The supernatants were centrifuged at 10,000*g* for 15 minutes at 4°C, and the pellets were collected as the heavy membrane fractions. The supernatants were then centrifuged at 100,000*g* for 45 minutes at 4°C and collected as the cytosolic fraction. The activities of caspase-9 and caspases-3/7 were measured using Ac-LEHD-AFC or Ac-DEVD-AFC (Enzyme Systems Products, Livermore, CA) as substrates, respectively. The substrates were preincubated for 10 minutes at 37°C in reaction buffer.[6] Thereafter, 100 μg of lysate was added to 1.25 mL of the substrate reaction buffer and incubated for 60 minutes at 37°C. The fluorescence of the released 7-amino-4-trifluoromethylcoumarin was detected using a fluorescence spectrometer (μQUANT; Bio-tech Instruments, Winooski, VT), with excitation at 400 nm and emission at 505 nm. One unit of caspase activity corresponds to the activity required to cleave 1 pmol of the substrate in 60 minutes at 37°C.

Colony Formation Assay

The colony formation assay was performed by the methylcellulose membrane method, as described previously.[7,8] Briefly, splenocytes were isolated from mice, plated at 4×10^5 cells/mL in 1% methylcellulose culture medium (Methocult 3430; StemCell Technology, Vancouver, Canada) that contained 100 μL of Iscove's modified Dulbecco's medium (Invitrogen, Carlsbad, CA) with 25 μg/mL of stem cell factor (R&D Systems, Minneapolis, MN) and hemin (Sigma-Aldrich, St. Louis, MO). Cells were infected with adenovirus that expressed the cre DNA recombinase (AxCANCre) or LacZ (AxCALacZ) gene and treated with cytokines (IL-2, IL-10, IL-12, and combinations thereof). Erythroid burst-forming units, as well as granulocyte, erythrocyte, macrophage, and megakaryocyte colony-forming units, and granulocyte/macrophage colony-forming units were measured.[7,8] To purify the $CD4^+$, $CD8^+$, and $CD45R/B220^+$ cell populations, peritoneal lymph node cells were isolated using immunomagnetic beads conjugated to the corresponding antibodies (Miltenyi Biotec, Bergisch Gladbach, Germany), as described previously.[9] In our series, >95% of the purified cells expressed the indicated phenotypes, and viability was >98%.[10] Colony numbers were counted at 7, 14, and 28 days posttreatment. Colonies that contained more than 30 cells were counted under sealed codes, which obscured the identities of the samples.

Antibody Coating and Cell Stimulation

The cell stimulation experiments adhered to the published protocols.[11] The following purified monoclonal antibodies were used in the cell stimulation experiments: anti-core, anti-E1, anti-E2 (Biodesign International, Saco, MN), and anti-His6 (Qiagen, Hilden, Germany). Ninety-six–well plates were coated with the various antibodies according to published methods.[11] For the experiments involving the blocking anti-core, E1, and E2 antibodies, the recombinant proteins were first treated with the blocking antibodies at 37°C for 30 minutes. The cells were then added to the core-, E1-, E2-, or antibody-coated plates, as previously described.[12]

Statistical Analysis

Data are presented as mean ± SD. Differences were compared using the Student *t* test and considered statistically significant at $P < .05$.

Supplementary Results

Inhibition of Fas-Induced Apoptosis by Disruption of irf-1 *Leads to Persistent Expression of HCV in Transgenic Mouse Livers*

The Fas ligand is essential for the development of hepatitis via cytotoxic T-lymphocyte–mediated cell killing.[13] Therefore, we determined the sensitivity of *irf-1*$^{-/-}$ hepatocytes to Fas-induced apoptosis. The *irf-1*$^{-/-}$ mice and WT littermates were injected intravenously with an anti-Fas monoclonal antibody. All 10 *irf-1*$^{-/-}$ mice survived, whereas 4 of 10 WT littermates died within 24 hours due to acute liver failure associated with massive hepatic apoptosis and hemorrhagic necrosis ($P < .05$; Supplementary Figure 2*A*). Acute and severe liver injury was confirmed by measurement of the serum ALT levels, which were increased by up to 200-fold in WT mice within 3 hours of administration of the anti-Fas monoclonal antibody (Supplementary Figure 2*B*). In contrast, delayed and less prominent increases in serum ALT levels were observed in the *irf-1*$^{-/-}$ mice 3 hours and 6 hours after injection of the anti-Fas monoclonal antibody (Supplementary Figure 2*B*). The WT mice had severe lesions of the liver, and staining with 4′,6-diamidino-2-phenylindole revealed morphologic changes that were characteristic of apoptosis (Supplementary Figure 2*C*). Massive panlobular and multilobular apoptotic necrosis (>90%) and peliosis were observed in the *irf-1*$^{-/-}$ CN2 mice in conjunction with 20% mortality (Supplementary Figure 2*C* [*a* and *b*]). Staining using TUNEL showed significantly lower levels of Fas-induced DNA fragmentation in the *irf-1*$^{-/-}$ hepatocytes than in the WT hepatocytes

(compare Supplementary Figure 2*C* [*i* and *j*]), and the onset of DNA fragmentation in *irf-1*$^{-/-}$ hepatocytes was delayed compared with that in WT hepatocytes (data not shown). There were no significant injuries to other organs, such as the thymus and kidneys. Thus, the WT mice showed severe, acute Fas-induced hepatic cytolysis, whereas the *irf-1*$^{-/-}$ mice had significantly delayed serum ALT production and lower serum ALT levels, along with delayed and less severe apoptosis of liver cells, indicating that disruption of *irf-1* inhibits the Fas-induced apoptosis of hepatocytes in vivo.

Several caspases, especially caspase-7 and caspase-3, are activated to cleave cytoplasmic and cytoskeletal proteins during Fas-induced apoptosis of murine hepatocytes.[14,15] To determine the mechanism by which disruption of *irf-1* inhibits Fas-induced apoptosis of hepatocytes, we examined caspase mRNA expression in ribonuclease protection assays. The levels of caspase-1 mRNA in *irf-1*$^{-/-}$ hepatocytes were significantly lower than those in WT hepatocytes, which is in agreement with previously reported results.[16] Interestingly, the caspase-6 and caspase-7 mRNA levels were also lower in the *irf-1*$^{-/-}$ mice than in the WT mice (Supplementary Figure 2*D* and *E*). The disruption of *irf-1* did not affect the levels of Fas or protein kinase R protein (data not shown). Furthermore, the anti-Fas monoclonal antibody induced the release of comparable levels of cytochrome *c* from the mitochondria to the cytoplasm in the WT and *irf-1*$^{-/-}$ hepatocytes (data not shown). These results suggest that the reduced expression of effector caspases may delay Fas-mediated apoptosis in *irf-1*$^{-/-}$ mice and abrogate the elimination of HCV-expressing cells in vivo.

Supplementary Discussion

HCV-infected patients have elevated levels of serum IL-10 and IL-12.[17] As shown in the present study, altered cytokine production may enhance HCV-induced lymphoproliferation. IL-10-transgenic mice develop Fas ligand–mediated exocrinopathy that resembles Sjögren's syndrome.[18] This exocrinopathy was also observed in some of the HCV protein-expressing mice in the current study. Therefore, the induction of cytokine expression in HCV transgenic mice may trigger lymphomagenesis. The induction of the gene that encodes the p40 subunit of IL-12, which is essential for Th1-type differentiation of the immune system, is entirely dependent on IRF-1,[19,20] which indicates that *irf-1* disruption affects the production of IL-12. In addition, HCV core protein reportedly activates the promoter for IL-2,[21] which is a growth factor for antigen-stimulated T lymphocytes that is responsible for antigen-induced clonal expansion of T cells. The high serum concentrations of IL-2 and IL-10 may also accelerate the differentiation of memory B cells.[22] Moreover, the induction of splenocyte proliferation by treatment with IL-2 plus IL-10 was suppressed by IL-12 in *irf-1*$^{-/-}$ CN2 mice. This suggests a potential application of IL-12 therapy for lymphomas associated with HCV infection. Long-term HCV infection may result in clonal B-cell expansion of immunoglobulin-secreting lymphocytes; approximately 35% of HCV-infected patients are reported to develop B-cell lymphoma.[23] HCV infection is associated not only with non-Hodgkin's B-cell lymphoma, but also with other lymphoid and myeloid malignancies, including non-Hodgkin's T-cell lymphomas; this association is consistent with our findings, especially in the *irf-1*$^{-/-}$ HCV transgenic mouse model (Figures 3 and 6).[24–27] It is also worth clarifying whether and at what frequency polyclonal lymphoid hyperplasia precedes lymphomagenesis and whether progression from hyperplasia to lymphoma is heralded by a more striking impairment of cytokine (ie, IL-2, IL-10, or IL-12) production.

We found that Fas-induced apoptosis was significantly suppressed in *irf-1*$^{-/-}$ hepatocytes. This suppression may be related to the essential role that IRF-1 plays in the induction of caspase expression.[16,28] Almost all of the *irf-1*$^{-/-}$ CN2 mice persistently expressed higher levels of HCV core protein in the liver, as compared with the *irf-1*$^{+/+}$ CN2 mice, which suggests wither deficient immunity or inefficient induction of apoptosis in *irf-1*$^{-/-}$ lymphocytes and hepatocytes. Immune surveillance in *irf-1*$^{-/-}$ mice may not eliminate efficiently the HCV protein-expressing cells due to reductions in the numbers of natural killer[19] and CD8^{+} T cells.[9] Furthermore, IRF-1 is an essential mediator of IFN-γ–induced cell cycle arrest and apoptosis.[29] Because activated lymphocytes are normally eliminated by activation-induced cell death, we speculate that the inhibition of apoptosis of *irf-1*$^{-/-}$ lymphocytes results in the accumulation of these cells in the lymph nodes and spleen. HCV core protein also modulates the activities of IFN-induced transacting factors in the Jak/Stat signaling pathway.[30] In addition, a protein kinase R–binding domain polypeptide of the HCV NS5A protein relieves the blockade of the IRF-1 pathway, resulting in the induction of IRF-1–dependent antiviral effector genes.[31] HCV NS5A alone is sufficient to block both the activation of IRF-1 and the induction of an IRF-1–dependent cellular promoter by double-stranded RNA.[31] Therefore, blockade of the IRF-1 pathway by HCV infection may facilitate the persistent expression of HCV proteins in hepatocytes or lymphocytes, resulting in the inhibition of Fas-mediated apoptosis in *irf-1*$^{-/-}$ hepatocytes. Indeed, genetic abnormalities in the Fas pathway in humans or *lpr* mice cause an autoimmune lymphoproliferative syndrome.[32] Differential modulation of apoptosis sensitivity in CD95 type I and type II cells (hepatocytes and some T lymphocytes) has been established.[33,34] It is noteworthy that both T lymphocytes and hepatocytes have CD95 type II signaling. It is interesting that lymphomagenesis is dominant over liver tumor development. The molecular mechanism underlying this dominance remains unknown. Further molecular analysis will

enlighten the differential signaling pathways between hepatocytes and lymphocytes.

Overexpression of *bcl-2* in B-lymphoid cells causes autoimmune disease,[35] and *bcl-2* immunoglobulin-transgenic mice develop follicular lymphoproliferation.[36] Therefore, the aberrant expression of *bcl-2* in CN2 lymphocytes may be another factor that inhibits activation-induced cell death, leading to a predisposition for lymphoproliferative disorders. In support of this notion, HCV-infected patients express elevated levels of Bcl-2[37] and frequently carry the t(14;18) chromosomal translocation.[38] Suppression of cell death by full-length Bcl-2 requires phosphorylation of Ser70[39,40]; in line with this, our Western blot analysis revealed 2 Bcl-2 species in the enlarged lymph nodes of the HCV protein-expressing mice. Bcl-2 and Fas/APO-1 regulate distinct pathways related to lymphocyte apoptosis.[35] Thus, both mitochondrion-dependent and mitochondrion-independent pathways exist for the induction of apoptosis. The dominant pathway differs depending on the tissue type.[13,35] Therefore, Bcl-2 expression and *irf-1* disruption may synergistically inhibit the apoptotic response in lymphocytes. Indeed, the expression of HCV proteins, chronic inflammation, and predisposition to lymphoproliferative disorders were all enhanced in CN2 mice upon *irf-1* disruption. Collectively, these results suggest that HCV stimulates oncogenesis by multiple mechanisms. Although the loss of the *irf-1* alleles does not result in spontaneous tumor development in mice, it enhances dramatically the risk of tumors caused by the *c-Ha-ras* transgene or by *p53* nullizygosity,[41] suggesting that the loss of *irf-1* confers susceptibility to tumor formation.

It has been proposed that HCV-infected lymphocytes induce t(18;14) translocation, which may result in the overexpression of Bcl-2, and a second mutation (in the *myc* oncogene), which leads to the development of lymphoma.[42,43] Because the promoter region of Bcl-2 includes SP1, Cre, nuclear factor κB,[44] and Akt/protein kinase B,[45] the combination of core expression and IL-10 and/or IL-2 may up-regulate these transcription factors by integrating several different pathways.

Supplementary References

1. Wakita T, Taya C, Katsume A, et al. Efficient conditional transgene expression in hepatitis C virus cDNA transgenic mice mediated by the Cre/loxP system. J Biol Chem 1998;273:9001–9006.
2. Kashiwakuma T, Hasegawa A, Kajita T, et al. Detection of hepatitis C virus specific core protein in serum of patients by a sensitive fluorescence enzyme immunoassay (FEIA). J Immunol Methods 1996;190:79–89.
3. Miyanari Y, Atsuzawa K, Usuda N, et al. The lipid droplet is an important organelle for hepatitis C virus production. Nat Cell Biol 2007;9:1089–1097.
4. Duan H, Heckman CA, Boxer LM. Histone deacetylase inhibitors down-regulate bcl-2 expression and induce apoptosis in t(14;18) lymphomas. Mol Cell Biol 2005;25:1608–1619.
5. Machida K, Tsukiyama-Kohara K, Seike E, et al. Inhibition of cytochrome c release in Fas-mediated signaling pathway in transgenic mice induced to express hepatitis C viral proteins. J Biol Chem 2001;276:12140–12146.
6. MacFarlane M, Cain K, Sun XM, et al. Processing/activation of at least four interleukin-1beta converting enzyme-like proteases occurs during the execution phase of apoptosis in human monocytic tumor cells. J Cell Biol 1997;137:469–479.
7. Gao JL, Wynn TA, Chang Y, et al. Impaired host defense, hematopoiesis, granulomatous inflammation and type 1-type 2 cytokine balance in mice lacking CC chemokine receptor 1. J Exp Med 1997;185:1959–1968.
8. Cotterell SE, Engwerda CR, Kaye PM. Enhanced hematopoietic activity accompanies parasite expansion in the spleen and bone marrow of mice infected with Leishmania donovani. Infect Immun 2000;68:1840–1848.
9. Yokota T, Oritani K, Takahashi I, et al. Adiponectin, a new member of the family of soluble defense collagens, negatively regulates the growth of myelomonocytic progenitors and the functions of macrophages. Blood 2000;96:1723–1732.
10. Oritani K, Hirota S, Nakagawa T, et al. T lymphocytes constitutively produce an interferonlike cytokine limitin characterized as a heat- and acid-stable and heparin-binding glycoprotein. Blood 2003;101:178–185.
11. Crotta S, Stilla A, Wack A, et al. Inhibition of natural killer cells through engagement of CD81 by the major hepatitis C virus envelope protein. J Exp Med 2002;195:35–41.
12. Machida K, Cheng KT, Pavio N, et al. Hepatitis C virus E2-CD81 interaction induces hypermutation of the immunoglobulin gene in B cells. J Virol 2005;79:8079–8089.
13. Kondo Y, Sung VM, Machida K, et al. Hepatitis C virus infects T cells and affects interferon-gamma signaling in T cell lines. Virology 2007;361:161–173.
14. Jones TA, Jones SM. Short latency compound action potentials from mammalian gravity receptor organs. Hear Res 1999;136:75–85.
15. Collins CE, Quaggiotto P, Wood L, et al. Elevated plasma levels of F2 alpha isoprostane in cystic fibrosis. Lipids 1999;34:551–556.
16. Kim EJ, Lee JM, Namkoong SE, et al. Interferon regulatory factor-1 mediates interferon-gamma-induced apoptosis in ovarian carcinoma cells. J Cell Biochem 2002;85:369–380.
17. Kakumu S, Okumura A, Ishikawa T, et al. Production of interleukins 10 and 12 by peripheral blood mononuclear cells (PBMC) in chronic hepatitis C virus (HCV) infection. Clin Exp Immunol 1997;108:138–143.
18. Saito I, Haruta K, Shimuta M, et al. Fas ligand-mediated exocrinopathy resembling Sjogren's syndrome in mice transgenic for IL-10. J Immunol 1999;162:2488–2494.
19. Taki S, Sato T, Ogasawara K, et al. Multistage regulation of Th1-type immune responses by the transcription factor IRF-1. Immunity 1997;6:673–679.
20. Lohoff M, Ferrick D, Mittrucker HW, et al. Interferon regulatory factor-1 is required for a T helper 1 immune response in vivo. Immunity 1997;6:681–689.
21. Bergqvist A, Rice CM. Transcriptional activation of the interleukin-2 promoter by hepatitis C virus core protein. J Virol 2001;75:772–781.
22. Choi YS. Differentiation and apoptosis of human germinal center B-lymphocytes. Immunol Res 1997;16:161–174.
23. Galossi A, Guarisco R, Bellis L, et al. Extrahepatic manifestations of chronic HCV infection. J Gastrointestin Liver Dis 2007;16:65–73.
24. Mele A, Pulsoni A, Bianco E, et al. Hepatitis C virus and B-cell non-Hodgkin lymphomas: an Italian multicenter case-control study. Blood 2003;102:996–999.

25. Dietrich CF, Lee JH, Herrmann G, et al. Enlargement of perihepatic lymph nodes in relation to liver histology and viremia in patients with chronic hepatitis C. Hepatology 1997;26:467–472.
26. Ascoli V, Lo Coco F, Artini M, et al. Extranodal lymphomas associated with hepatitis C virus infection. Am J Clin Pathol 1998; 109:600–609.
27. Silvestri F, Pipan C, Barillari G, et al. Prevalence of hepatitis C virus infection in patients with lymphoproliferative disorders. Blood 1996;87:4296–4301.
28. Liu ZX, Govindarajan S, Okamoto S, et al. Fas- and tumor necrosis factor receptor 1-dependent but not perforin- dependent pathways cause injury in livers infected with an adenovirus construct in mice. Hepatology 2000;31:665–673.
29. Kano A, Haruyama T, Akaike T, et al. IRF-1 is an essential mediator in IFN-gamma-induced cell cycle arrest and apoptosis of primary cultured hepatocytes. Biochem Biophys Res Commun 1999;257:672–677.
30. Potapova O, Basu S, Mercola D, et al. Protective role for c-Jun in the cellular response to DNA damage. J Biol Chem 2001;276: 28546–28553.
31. Pflugheber J, Fredericksen B, Sumpter R Jr, et al. Regulation of PKR and IRF-1 during hepatitis C virus RNA replication. Proc Natl Acad Sci U S A 2002;99:4650–4655.
32. Sobel ES, Kakkanaiah VN, Kakkanaiah M, et al. Co-infusion of normal bone marrow partially corrects the gld T-cell defect. Evidence for an intrinsic and extrinsic role for Fas ligand. J Immunol 1995;154:459–464.
33. Scaffidi C, Fulda S, Srinivasan A, et al. Two CD95 (APO-1/Fas) signaling pathways. EMBO J 1998;17:1675–1687.
34. Scaffidi C, Schmitz I, Zha J, et al. Differential modulation of apoptosis sensitivity in CD95 type I and type II cells. J Biol Chem 1999;274:22532–22538.
35. Strasser A, Harris AW, Bath ML, et al. Novel primitive lymphoid tumours induced in transgenic mice by cooperation between myc and bcl-2. Nature 1990;348:331–333.
36. McDonnell TJ, Deane N, Platt FM, et al. bcl-2-immunoglobulin transgenic mice demonstrate extended B cell survival and follicular lymphoproliferation. Cell 1989;57:79–88.
37. Casato M, Mecucci C, Agnello V, et al. Regression of lymphoproliferative disorder after treatment for hepatitis C virus infection in a patient with partial trisomy 3, Bcl-2 overexpression, and type II cryoglobulinemia. Blood 2002;99:2259–2261.
38. Kitay-Cohen Y, Amiel A, Hilzenrat N, et al. Bcl-2 rearrangement in patients with chronic hepatitis C associated with essential mixed cryoglobulinemia type II. Blood 2000;96:2910–2912.
39. Ito T, Deng X, Carr B, et al. Bcl-2 phosphorylation required for anti-apoptosis function. J Biol Chem 1997;272:11671–11673.
40. Kuwata H, Watanabe Y, Miyoshi H, et al. IL-10-inducible Bcl-3 negatively regulates LPS-induced TNF-alpha production in macrophages. Blood 2003;102:4123–4129.
41. Nozawa H, Oda E, Nakao K, et al. Loss of transcription factor IRF-1 affects tumor susceptibility in mice carrying the Ha-ras transgene or nullizygosity for p53. Genes Dev 1999;13:1240–1245.
42. Zignego AL, Giannelli F, Marrocchi ME, et al. T(14;18) translocation in chronic hepatitis C virus infection. Hepatology 2000;31: 474–479.
43. Ellis M, Rathaus M, Amiel A, et al. Monoclonal lymphocyte proliferation and bcl-2 rearrangement in essential mixed cryoglobulinaemia. Eur J Clin Invest 1995;25:833–837.
44. Ma Q, Li X, Vale-Cruz D, Brown ML, et al. Activating transcription factor 2 controls Bcl-2 promoter activity in growth plate chondrocytes. J Cell Biochem 2007;101:477–487.
45. Pugazhenthi S, Nesterova A, Sable C, et al. Akt/protein kinase B up-regulates Bcl-2 expression through cAMP-response element-binding protein. J Biol Chem 2000;275:10761–10766.
46. Taniguchi T, Ogasawara K, Takaoka A, et al. IRF family of transcription factors as regulators of host defense. Annu Rev Immunol 2001;19:623–655.
47. Penninger JM, Sirard C, Mittrucker HW, et al. The interferon regulatory transcription factor IRF-1 controls positive and negative selection of CD8+ thymocytes. Immunity 1997;7:243–254.

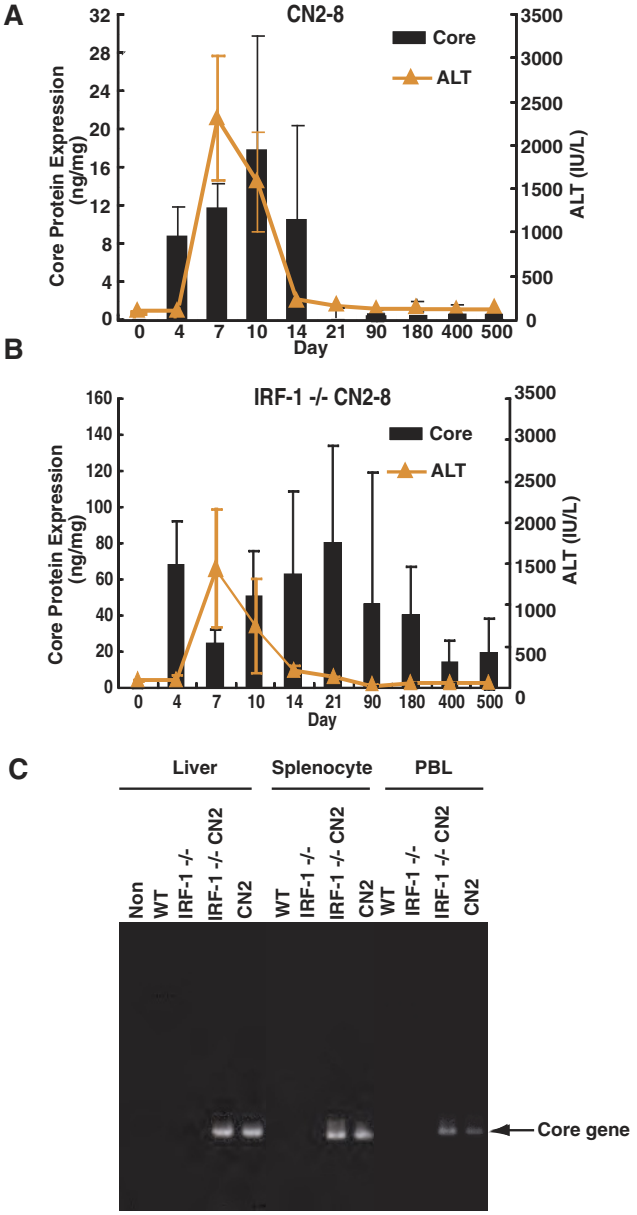

Supplementary Figure 1. (*A* and *B*) Levels of serum ALT and core protein expression in the hepatocytes of (*A*) CN2-8 and (*B*) *irf-1*$^{-/-}$ CN2-8 mice following the administration of AxCANCre (n = 225 for *irf-1*$^{-/-}$; n = 75 for *irf-1*$^{-/-}$ CN2-29; n = 150 for *irf-1*$^{-/-}$ CN2-8; n = 225 for WT; n = 75 for CN2-29; and n = 150 for CN2-8; total of 900 mice). (*C*) Expression levels of the HCV core gene in the liver, splenocytes, and peripheral blood lymphocytes of the WT, *irf-1*$^{-/-}$, *irf-1*$^{-/-}$ CN2, and CN2 mice, as determined by PCR.

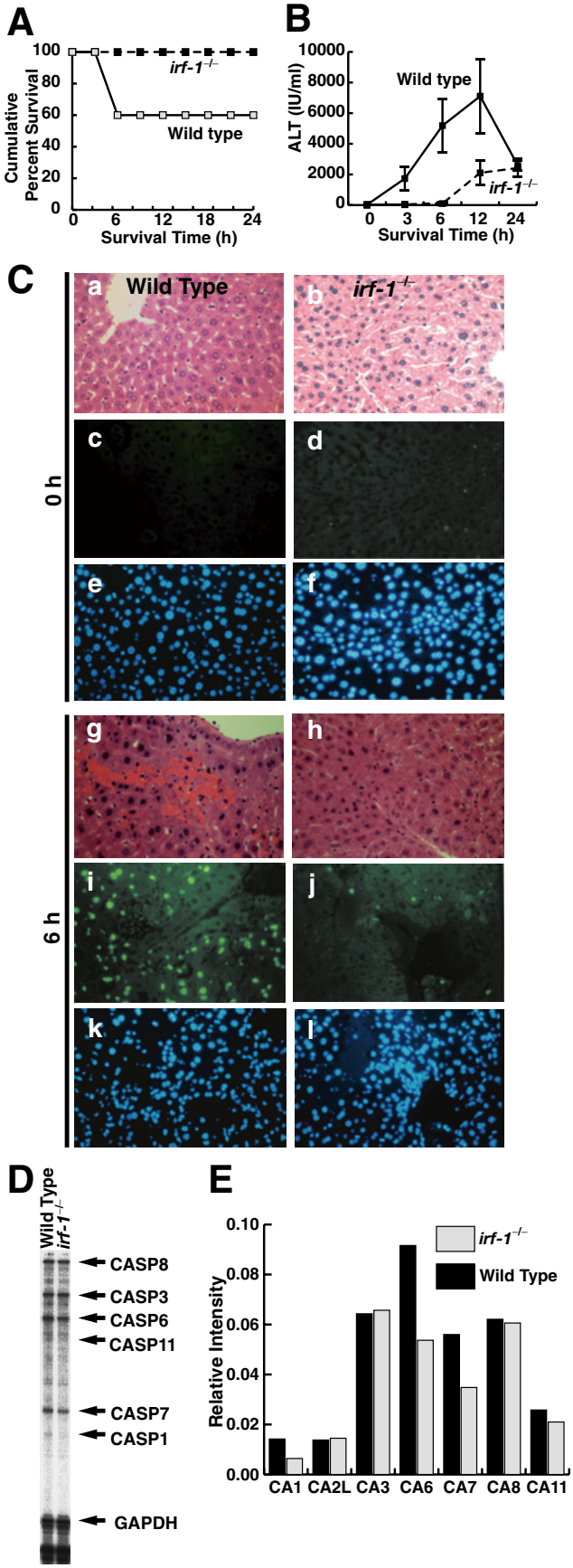

←

Supplementary Figure 2. Disruption of *irf-1* allows persistent expression of HCV proteins and inhibits Fas-induced apoptosis. The percentages of survivors 24 hours after injection of the anti-Fas monoclonal antibody into *irf-1*$^{+/+}$ and *irf-1*$^{-/-}$ mice. Serum ALT levels in *irf-1*$^{-/-}$ and *irf-1*$^{+/+}$ mice following anti-Fas monoclonal antibody injection. Histology of livers from *irf-1*$^{-/-}$ CN2 and *irf-1*$^{+/+}$ (WT) mice following injection of the anti-Fas monoclonal antibody. (*a*, *b*, *g*, and *h*) Liver sections stained with H&E 6 hours after injection of the anti-Fas monoclonal antibody (original magnification 40×). (*c*, *d*, *i*, and *j*) Apoptotic cells in the liver tissues identified by TUNEL staining 6 hours after injection of the anti-Fas monoclonal antibody. (*e*, *f*, *k*, and *l*) Nuclear staining with 4′,6-diamidino-2-phenylindole of liver sections from WT and *irf-1*$^{-/-}$ mice. The levels of expression of caspases -1, -2A, -3, -6, -7, -8, and -11 and control (glyceraldehyde-3-phosphate dehydrogenase) transcripts were determined in an ribonuclease protection assay using hepatocyte RNA species from WT and *irf-1*$^{-/-}$ mice. Relative intensities of caspase mRNA expression in the hepatocytes of the WT and *irf-1*$^{-/-}$ mice, with normalization for the expression of *GAPDH*.

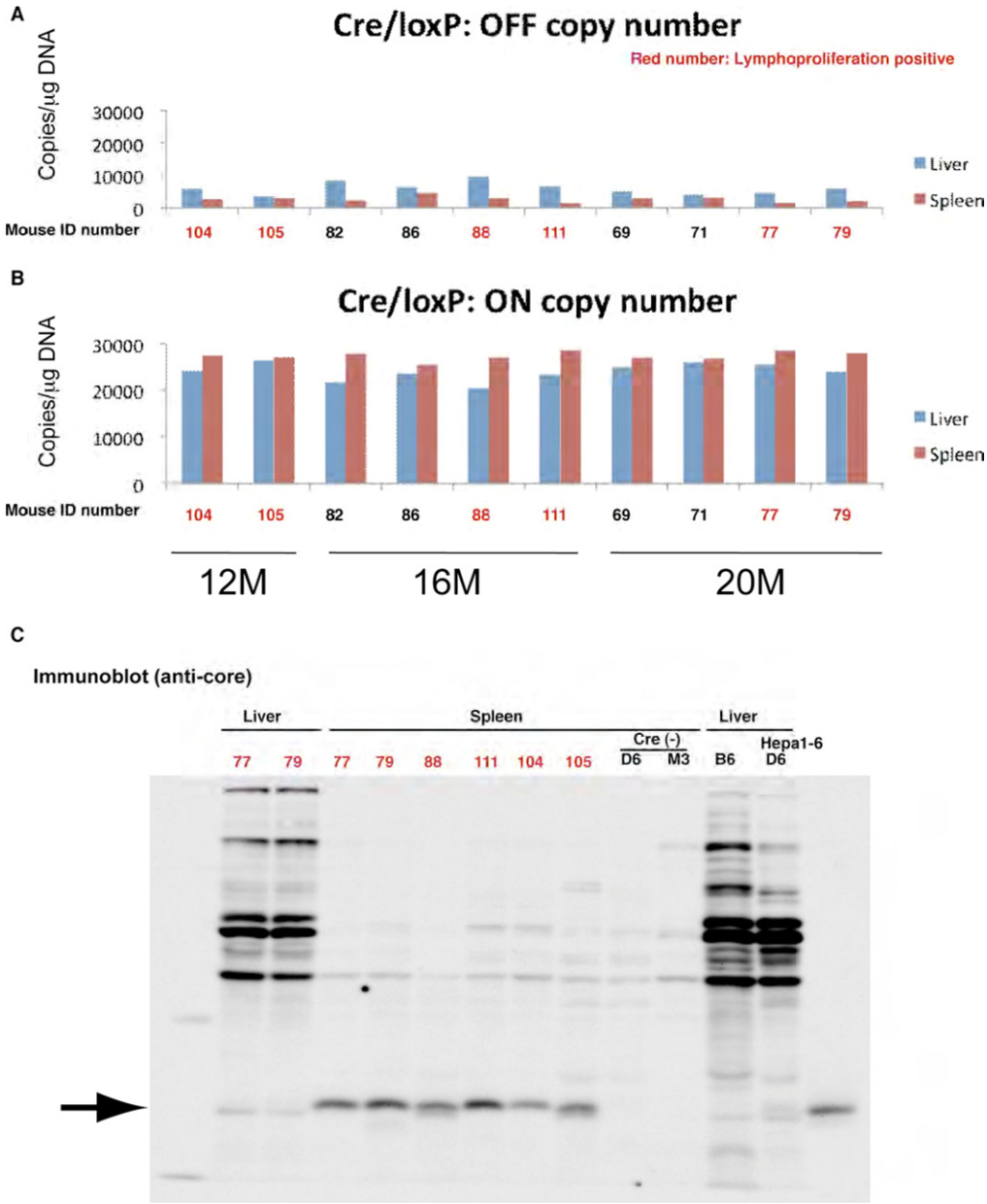

Supplementary Figure 3. Switching efficiency for the expression of the HCV transgene using quantitative real-time PCR. (*A* and *B*) Viral gene expression levels were examined by quantitative real-time PCR before and after poly(I:C) injection. (*C*) Representative immunoblot for the detection of HCV core protein expression in murine livers and spleens.

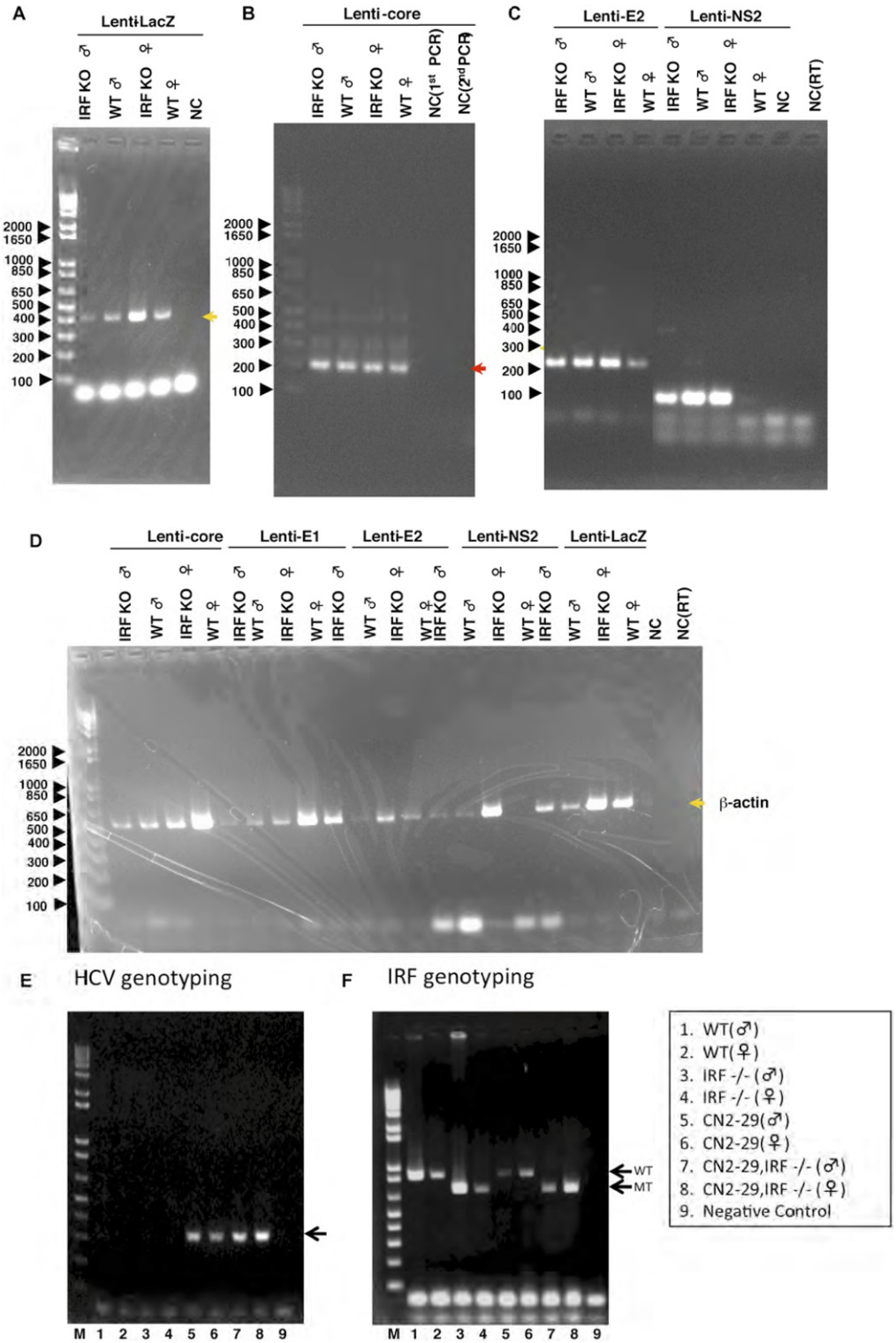

Supplementary Figure 4. Real-time PCR for HCV transgene expression. (*A–D*) The HCV gene expression levels in splenocytes transfected with lentiviral vectors were examined by real-time PCR. Lentiviruses that expressed (*A*) LacZ, (*B*) core, and (*C*) E2 and NS2 were used to infect the splenocytes. The mRNA expression levels were detected by real-time PCR. (*D*) The real-time PCR of *β-actin* serves as a control. (*E*) Representative agarose gel images for the genotyping of HCV transgenes and *irf-1*.[17]

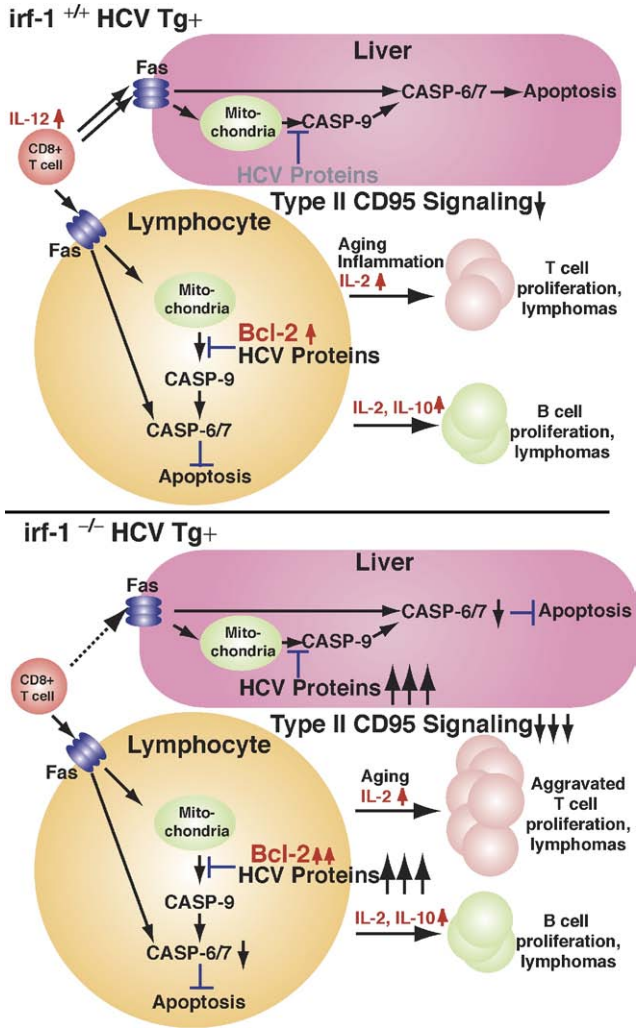

Supplementary Figure 5. Hypothetical model for the triggering of oncogenic potential by disruption of *irf-1* in synergy with HCV transgene expression. The levels of Bcl-2 and cytokines, as well as aging and inflammation, may enhance the development of lymphoproliferative disorders caused by HCV proteins. Disruption of *irf-1* enables the persistent expression of HCV proteins, leading to lymphoproliferative disease due to reduced apoptosis (ie, lower expression of caspase-1, -6, and -7). HCV CN2 transgenic (Tg+) mice are resistant to Fas-induced apoptosis due to inhibition of cytochrome *c* release from the mitochondria.[5] Mice with disruption of the *irf-1* gene have several defects of the innate and adaptive immunity systems, such as lineage-specific defects in thymocyte development, whereby immature T cells can develop into mature $CD4^+$ cells but not into $CD8^+$ T cells.[19,46] IRF-1 controls the positive and negative selection of $CD8^+$ thymocytes.[47] IRF-1 is required for the development of the Th1-type immune response, and its absence leads to the induction of the Th2-type immune response.[19,20] The number of natural killer cells is dramatically reduced in the *irf-1*$^{-/-}$ mice.[19] Expression of the IL-12 p40 subunit is defective in *irf-1*$^{-/-}$ mice.[19] In the present study, mice with persistent expression of HCV proteins had elevated serum levels of IL-2, IL-10, and IL-12 and higher levels of Bcl-2 protein in enlarged lymph nodes, and these phenomena were more pronounced in the absence of IRF-1.

Supplementary Table 1. Mouse Strains and Viral Protein Functions

Viral protein	Function	CN2-8 mouse strain		CN2-29 mouse strain	
Core	Nucleocapsid	Cre/loxP	Expressed	Cre/loxP	Expressed
E1	Envelope	Switching	Expressed	Switching	Expressed
E2	Envelope	On/off	Expressed	On/off	Expressed
NS2	Proteinase	Regulation	Expressed	Regulation	Expressed